Journal of Power Sources 241 (2013) 751–755

Contents lists available at SciVerse ScienceDirect

Journal of Power Sources

journal homepage: www.elsevier.com/locate/jpowsour

Short communication

A new kind of highly active hollow flower-like NiPdPt nanoparticles supported by multiwalled-carbon nanotubes toward ethanol electrooxidation

Wei Hong [a,b], Yaqing Liu [a,*], Jin Wang [a,c,*], Erkang Wang [a,b]

[a] State Key Laboratory of Electroanalytical Chemistry, Changchun Institute of Applied Chemistry, Chinese Academy of Sciences, Changchun 130022, China
[b] University of Chinese Academy of Sciences, Beijing 100039, China
[c] Department of Chemistry and Physics, State University of New York at Stony Brook, New York, NY 11794-3400, USA

HIGHLIGHTS

- Carbon-supported hollow flower-like NiPdPt has been synthesized.
- Ni nanoparticles are used as the sacrificial template to obtain NiPdPt.
- NiPdPt are well assembled on carbon nanotubes through electrostatic interaction.
- The as-prepared catalysts exhibit excellent electrocatalytic activity.

ARTICLE INFO

Article history:
Received 8 March 2013
Received in revised form
11 May 2013
Accepted 17 May 2013
Available online 28 May 2013

Keywords:
Nickel
Palladium
Platinum
Hollow flower-like
Multiwalled-carbon nanotubes
Ethanol electrooxidation

ABSTRACT

Hollow flower-like NiPdPt nanoparticles (NPs) are prepared through galvanic replacement between Ni nanoparticles and noble metal salts. Multiwalled-carbon nanotubes (MWCNTs) can be used to support the as synthesized hollow flower-like NiPdPt NPs through electrostatic self-assembly. The structure and composition are analyzed by transmission electron microscope, X-ray diffraction and inductively coupled plasma optical emission spectrometer. Electrochemical catalytic measurement results prove that the as synthesized MWCNTs supported NiPdPt NPs present excellent catalytic activity toward ethanol electrooxidation in alkaline solution.

1. Introduction

In recent years, fuel cells have been receiving increasing attentions taking the advantages of its high efficiency and cleanness [1]. Direct ethanol fuel cells (DEFCs) are attracting special attention owing to its wide application nowadays, such as power sources for portable electronic devices and fuel-cell vehicles etc [2]. Comparing with other direct fuel cells, DEFCs present many obvious advantages. First, ethanol can be easily obtained in large quantities from chemical industry and fermentation of biomass. Second, ethanol has a lower toxicity while provides a higher energy density compared to its counterparts such as methanol and formic acid. Moreover, DEFCs conducting in alkaline media have some other obvious advantages such as improved kinetics for low-overvoltage ethanol oxidation and reduced risk of corrosion of the materials for high durability [3–5]. However, a significant challenge in the development of DEFCs technology is the urgent need for highly active catalysts for the ethanol oxidation reaction which takes place at the negative electrode [6].

Pd-based catalysts have been proven to be promising candidates for DEFCs due to its good catalytic activity and relatively low cost

* Corresponding authors. State Key Laboratory of Electroanalytical Chemistry, Changchun Institute of Applied Chemistry, Chinese Academy of Sciences, Changchun 130022, China. Fax: +86 43185689711.
E-mail addresses: yaqingliu@ciac.jl.cn (Y. Liu), jin.wang.1@stonybrook.edu (J. Wang).

0378-7753/$ – see front matter © 2013 Published by Elsevier B.V.
http://dx.doi.org/10.1016/j.jpowsour.2013.05.072

[5,7]. Many previous studies validate that the shape, size and composition of nanoparticles, have a significant effect on its catalytic activity [8,9]. Rationally design of bimetallic or multi-metallic nanostructures has been one of the hottest and attractive research topics for improving its catalytic activity and utilization efficiency of noble metals [10–12]. Until now, a variety of Pd-based materials have been synthesized for DEFCs, such as TiO_2 nanotubes supported-Pd [13], carbon-supported PdM (M = Au and Sn) nanocatalysts [14], carbon-supported PdSn binary catalysts [15] and Pd–Ni electrocatalysts [16,17], water-dispersible hybrid Au–Pd nanoparticles [18], carbon-supported Pd–Ag [19], Pt/Pd bimetallic nanotubes [2] and PdM (M = Pt, Au) bimetallic alloy nanowires etc [20]. Among these materials, PtPd materials draw particular attention by virtue of their outstanding catalytic activity derived from the presence of the powerful catalytic components of Pt and Pd [21].

As a special structure, metallic hollow nanospheres exhibit higher catalytic activity with the advantages of low density, saving materials, and reduction of costs compared with their solid counterparts [22–24]. Despite of some methods have already been developed for the synthesis of metallic hollow structure, it remains a great challenge to develop a one-pot and general route for the preparation of metallic hollow nanostructures. Hard templates methods still remain the most powerful and versatile way to prepare metallic hollow nanostructure. Among those cases, Co and Ag nanoparticles are two of the most often used sacrificial templates to obtain noble metallic hollow structure. However, Ag templates are not favorable from the point view of economy due to its relatively high price. What's more, employing Ag templates always lead to the AgCl precipitates and thus the further removal procedures [25,26]. Co templates are more economic comparing with Ag templates. However, it exhibits strong magnetic force, which may lead to adhesion and even aggregation of metallic hollow structure [27]. Compared with that, Ni as a non-noble metal, is more economical than Ag templates. Meanwhile, it has a weaker magnetic force than Co templates. What's more, the presence of Ni in Pd and Pt were found to be very favorable for the improvement of catalytic performance, due to the synergistic effect between small amount of Ni and Pt/Pd, which can greatly enhance the catalytic activity and stability of the catalyst [6].

In this work, we successfully developed a method to synthesize multiwalled-carbon nanotubes supported NiPdPt nanoparticles (MWCNTs-NiPdPt) by the galvanic replacement, employing Ni nanoparticles as the sacrificial templates. The obtained MWCNTs-NiPdPt were characterized with X-ray diffraction (XRD), transmission electron microscopy (TEM), inductively coupled plasma optical emission spectrometer (ICP-OES). The catalytic activity and stability of the prepared catalysts were investigated by cyclic voltammetry and chronoamperometry methods in alkaline media.

2. Experimental

2.1. Materials

Multiwalled-carbon nanotubes were purchased from Shenzhen Nanotech Port Company (China) and purified by refluxing in 3 mol L^{-1} nitric acid for 24 h. Vulcan XC-72 carbon was bought from Shanghai Ouman Chemical Corp (Shanghai, China). Nafion ethanol solution (5 wt.%) was obtained from Aldrich. Commercial ETK-Pd/C was purchased from Alfa Aesar. Sodium tetrachloropalladate (II), potassium chloroplatinate and trisodium citrate were obtained from Beijing Chemical Corp (China). All chemicals used were of analytical grade and used without further purification. Milli-Q ultrapure water (Millipore, ≥18.2 MΩ cm) was used throughout the experiments.

2.2. Synthesis of hollow flower-like NiPdPt nanoparticles

To synthesize the sacrificial Ni nanoparticles, 0.8 mL 0.1 mol L^{-1} $NiCl_2$ was added into 50 mL deionized water, followed by adding 1 mL 0.2 mol L^{-1} trisodium citrate as the stabilizers. The mixed solution was purged with N_2 for 30 min, then 6 mL aqueous solution containing 5 mg $NaBH_4$ was added dropwise under vigorous stirring. After several minutes, 300 μL 0.0558 mol L^{-1} Na_2PdCl_4 and 870 μL 0.0193 mol L^{-1} K_2PtCl_6 together with water were mixed to a total volume of 7 mL, and sequentially added to the reaction solution slowly. For comparison, the different mole ratio of NiPdPt were also prepared, just by changing the volume of Na_2PdCl_4 to 450 μL, 300 μL and the volume of K_2PtCl_6 to 430 μL, 2.6 mL respectively. The final products were centrifuged and washed with water several times, and dissolved in water for further use.

2.3. Preparation of MWCNTs-NiPdPt catalysts

4 mg of the as treated MWCNTs were dissolved in 6 mL water. To the solution, 100 μL poly(diallyldimethylammonium chloride) (PDDA) (25%) were added and sonicated for 3 h. The solution was then centrifuged and washed with water to remove the excessive PDDA. Subsequently, the MWCNTs were dissolved in 6 mL water, then mixed with half of the above prepared hollow flower-like NiPdPt nanoparticles and stirred overnight. Finally, the products were centrifuged and concentrated for further structural, composition and electrochemical characterizations. The Vulcan XC-72 carbon-supported $NiPd_{20}Pt_{23}$ was prepared by mixing carbon and $NiPd_{20}Pt_{23}$ together and sonicated for 15 min, then stirred overnight. The final products were centrifuged and concentrated.

2.4. Material structure and composition characterizations

The morphology and structure of the as prepared catalysts were analyzed with a HITACHI H-600 Analytical TEM with an accelerating voltage of 100 kV. The exact composition of MWCNTs-NiPdPt was determined by ICP-OES (X Series 2, Thermo Scientific USA). XRD pattern of MWCNTs-NiPdPt was performed on a D8 ADVANCE (BRUKER, Germany) diffractometer using Cu-Kα radiation with a Ni filter ($\lambda = 0.154059$ nm at 30 kV and 15 mA).

2.5. Electrochemical catalytic test toward ethanol electrooxidation

For electrochemical catalytic test, a glassy carbon electrode (GCE) with a diameter of 2.5 μm was employed as working electrode. A platinum wire was used as the counter electrode with Ag/AgCl electrode as the reference electrode respectively. The voltage applied has been converted to the voltage referenced to normal hydrogen electrode (NHE). Before each experiment, the GCE was polished carefully with 1.0, 0.3, and 0.05 μm alumina powder and rinsed with deionized water, followed by sonication in ethanol and Milli-Q ultrapure water successively. Then, the electrode was dried under nitrogen. For electrooxidation of ethanol test, 5 μL of commercial ETK-Pd/C or MWCNTs-NiPdPt catalysts solution (0.5 mg mL^{-1} of metal) was dropped on the surface of the GC electrode and dried with an infrared lamp carefully. Then, 5 μL of Nafion (0.5%) was coated on the surface of the above material modified GCE and dried before electrochemical experiments. All the electrochemical tests were carried out on a CHI 832B electrochemical workstation, Chenhua Instruments Corp (Shanghai, China).

3. Results and discussion

3.1. TEM, XRD and ICP-OES characterizations of the MWCNTs-NiPdPt catalysts

Fig. 1a shows the typical TEM images of the prepared hollow flower-like NiPdPt nanoparticles. It can also be noted in the TEM images of Fig. 1b that there is few broken nanoparticles, so the prepared nanoparticles cannot be core-shell structures. The inserted diagram in Fig. 1a presents the size distribution of the prepared NiPdPt nanoparticles. The average size of the particles is about 21.7 nm. Fig. 1b presents the TEM image of the MWCNTs-NiPdPt catalysts, the image clearly shows that NiPdPt nanoparticles were well assembled on the multiwalled-carbon nanotubes. Since trisodium citrate stabilized NiPdPt nanoparticles are negatively charged while PDDA protected MWCNTs are positively charged, they can be well assembled through electrostatic interaction. Fig. 1b clearly proved that the electrostatic self-assembly is an effective way for nanostructure construction.

Fig. 2 presents the X-ray diffraction (XRD) pattern of the as prepared sample. The broadening of diffraction peak around 25° is ascribed to the graphite (002) facets of MWCNTs supports [6]. There are four characteristic diffraction peaks corresponding to (111), (200), (220) and (311) planes of the fcc structure respectively ascribed to the Pd and Pt. The two small peaks at 2 theta values of about 33.5° and 59.2° are attributed to $Ni(OH)_2$ (100) and (110) facets, respectively. The peaks of Ni in XRD pattern are weak due to its low content in the prepared NiPdPt nanoparticles. The same results can also be found in the reported literature [6,28].

The exact composition of as prepared catalysts was determined by ICP-OES and calculated to the mole ratio. The weight of Pd and Pt ($m_{metal} = m_{Pd} + m_{Pt}$) was also calculated exactly according to the ICP-OES measurement results and used to compare with that of commercial ETK-Pd/C during the electrochemical measurements.

3.2. Electrochemical measurements of MWCNTs-NiPdPt and ETK-Pd/C catalysts

The catalytic activity of the as prepared MWCNTs-NiPdPt toward ethanol electrooxidation in alkaline condition was evaluated with an electrochemical measurement system and compared with that of commercial ETK-Pd/C. Mass activity was used to evaluate the catalytic activity of the catalysts. Electrooxidation toward ethanol was carried out in aqueous solution containing 0.5 mol L^{-1} sodium hydroxide and 1 mol L^{-1} ethanol, using cyclic voltammetry (CV) measurements technique, sweeping from −0.58 V to 0.62 V at a

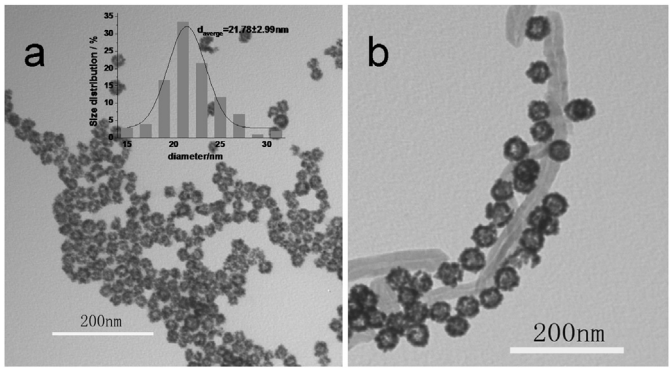

Fig. 1. (a) Typical TEM images of the as-prepared NiPdPt nanoparticles, the inserted diagram presents the size distribution of the prepared NiPdPt nanoparticles and (b) TEM images of multiwalled-carbon nanotubes supported NiPdPt nanoparticles.

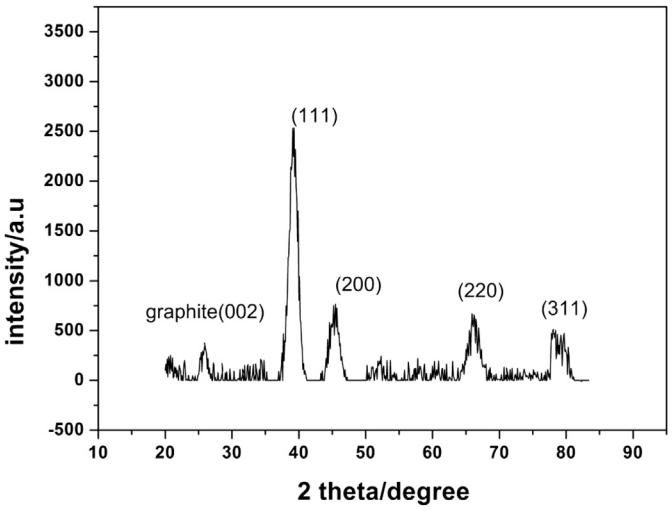

Fig. 2. XRD patterns of MWCNTs-NiPdPt.

scan rate of 50 mV s^{-1}. Fig. 3A shows the mass activity of the prepared catalysts and commercial ETK-Pd/C toward ethanol electrooxidation. The forward anodic peak of MWCNTs-$NiPd_{20}Pt_{23}$ is 3.01 A mg^{-1}_{metal}, 3.67 times of commercial ETK-Pd/C of 0.82 A mg^{-1}_{metal} as illustrated in Fig. 3A. The results is also higher than 1.16 A mg^{-1}_{metal} of Pt/Pd bimetallic nanotubes [2] and 0.95 A mg^{-1}_{metal} of PdPt alloy nanowires reported by Dong's group [11], indicating that the as prepared MWCNTs-$NiPd_{20}Pt_{23}$ possess an excellent catalytic activity. Learned from Fig. 3A, it also can be found that the peak value in backward scan of MWCNTs-$NiPd_{20}Pt_{23}$ is 2.23 A mg^{-1}_{metal} and is also much higher than commercial ETK-Pd/C of 0.6 A mg^{-1}_{metal}. To investigate the optimum ratio of NiPdPt with the best catalytic activity, another two types of MWCNTs-NiPdPt with different composition were prepared. The mass activity of each types were presented in Fig. 3C. It can be noted that peak current value of MWCNTs-$NiPd_{20}Pt_{23}$ is higher than both MWCNTs-$NiPd_{23}Pt_7$ and MWCNTs-$NiPd_{12}Pt_{43}$. The results suggest that the mole ratio between Pd and Pt of about 1:1 possess the best electrocatalytic activity toward ethanol electrooxidation. The results were consistent with PdPt alloy nanowires with different mole ratio [20]. We can also find from Fig. 3A and C that peak ethanol electrooxidation potential of MWCNTs-$NiPd_{20}Pt_{23}$ located between MWCNTs-$NiPd_{12}Pt_{43}$ and MWCNTs-$NiPd_{23}Pt_7$, and similar for commercial ETK-Pd/C and reported literature [33]. The reason for this results may be derived from the intrinsic mechanism for ethanol oxidation of different metals. A dual-path mechanism for ethanol oxidation in alkaline media was proposed by Tripkovic [29] and Koper [30,31]. The overall oxidation current will be determined by the sum of the oxidation current of the CH_3CO_{ads} and CO_{ads}. For the Pt, the oxidation current of ethanol can be contributed via both the C1 pathway and the C2 pathways. Since the oxidation of CO_{ads} species might have more stringent conditions for active sites than the oxidation of CH_3CO_{ads} species [30,31], the C1 pathway is much slower than the C2 pathway. Thus lead to the restricted kinetics of ethanol oxidation reaction and reflected by the higher onset potential of ethanol oxidation [31,32]. Moreover, it can also be further confirmed in Fig. 3C, that with the increase of Pt ratio in the NiPdPt, the peak ethanol electrooxidation potential changed to higher potential. For the Pd, however, the amount of C1 species on the Pd surface is much less than that on the Pt, therefore, only the oxidation current from the C2 pathway will be considered [32]. And it is generally believed that a CH_3CO_{ads} intermediate is formed on the Pd catalyst in the alkaline medium,

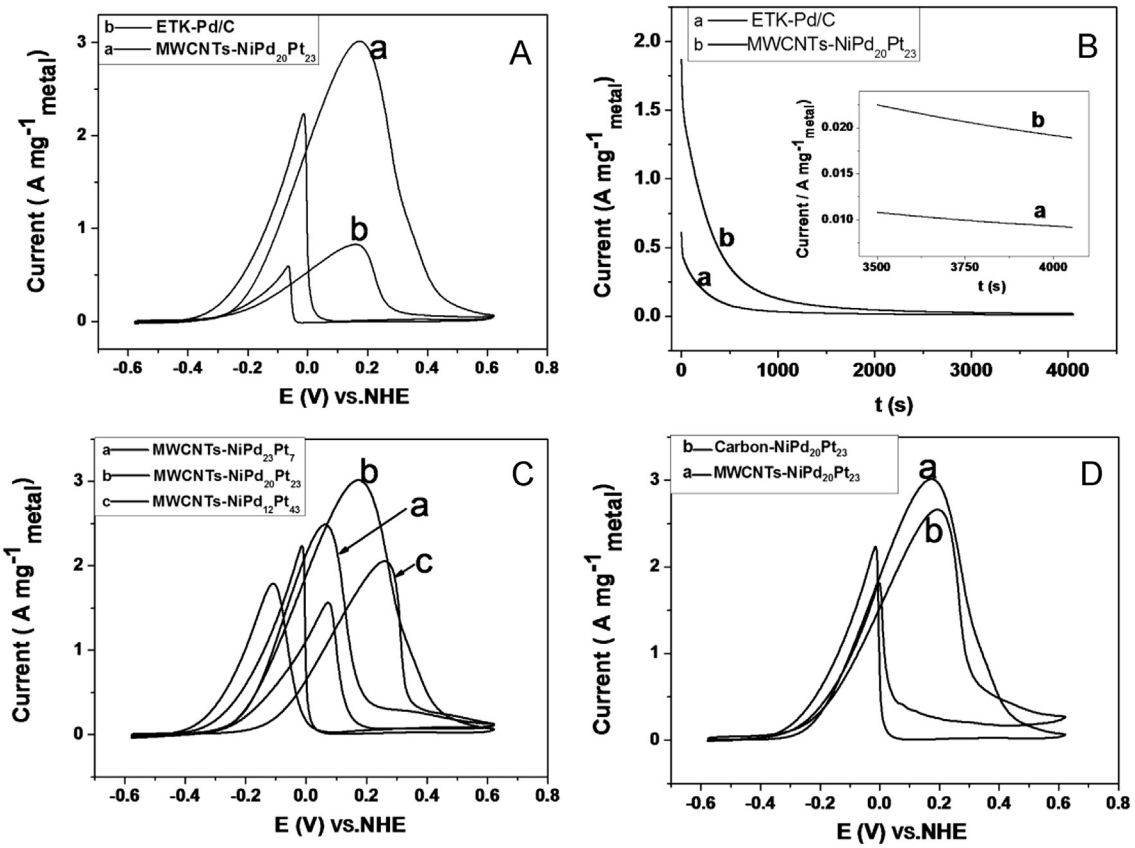

Fig. 3. (A) Mass activity of MWCNTs-$NiPd_{20}Pt_{23}$ and commercial ETK-Pd/C toward ethanol electrooxidation. (B) Current–time curve recorded at 0.022 V in solution containing 1 mol L^{-1} ethanol + 0.5 mol L^{-1} sodium hydroxide. (C) Mass activity of MWCNTs-NiPdPt with different composition toward ethanol electrooxidation. (D) Mass activity of $NiPd_{20}Pt_{23}$ supported on MWCNTs-$NiPd_{20}Pt_{23}$ and Vulcan XC-72 carbon toward ethanol electrooxidation.

and its reaction with OH_{ads} is the rate-determining step [34]. The co-metals Pt and small amount of Ni on the Pd provide their respective opportunities for activating the surface with the formation of OH_{ads} through synergistic effect. The special structure of the as prepared nanomaterials also makes a great contribution to the improvement of the catalytic activity. On one hand, the rough outer surface and porous shell can increase the active surface area thus the corresponding catalytic activity. On the other hand, the hollow metallic nanostructure takes advantage of saving materials and also play an important role to increase the mass activity performance. Meanwhile, MWCNTs have been proved to be excellent carbon support due to its unique and structure-dependent mechanical and electronic properties [35], which is conducive to enhance the catalytic performance. Fig. 3D show mass activity of $NiPd_{20}Pt_{23}$ supported on Vulcan XC-72 carbon and MWCNTs, the results clearly prove that MWCNTs play an important role in improving the catalytic activity of $NiPd_{20}Pt_{23}$.The above mentioned several features of the as prepared catalysts result in an outstanding electrochemical performance.

The stability of MWCNTs-$NiPd_{20}Pt_{23}$ toward ethanol electrooxidation was investigated by chronoamperometry technique at 0.022 V as illustrated in Fig. 3B. MWCNTs-$NiPd_{20}Pt_{23}$ nanoparticles show a distinct higher current value than ETK-Pd/C during the first 1500 seconds. However, both MWCNTs-$NiPd_{20}Pt_{23}$ and ETK-Pd/C show a sharp decrease current value. The phenomenon might be attributed to the formation of the oxide layer on the surface of electrode which can block the adsorption of the reactive species onto the Pd surface and lead to a decrease in the electrocatalytic activity [34]. Additionally, in regard to MWCNTs-$NiPd_{20}Pt_{23}$, the poison of Pt by CH_3CO_{ads} intermediates formed during the electrochemical process also cannot be ignored. After 4000 second, the residual current density of the MWCNTs-$NiPd_{20}Pt_{23}$ is 0.01917 A $mg^{-1}{}_{metal}$, still 2 times higher than 0.0092 A $mg^{-1}{}_{metal}$ of ETK-Pd/C (see the insert of Fig. 3B). It is clearly shown that the as-prepared MWCNTs-$NiPd_{20}Pt_{23}$ has a good tolerance toward ethanol electrooxidation. All the results confirm that MWCNTs-NiPdPt nanoparticles possess excellent catalytic performance toward ethanol oxidation in alkaline solution and present wide potential application for DEFCs in the future.

4. Conclusions

In conclusion, we successfully synthesized multiwalled-carbon nanotubes supported NiPdPt nanoparticles. Ni nanoparticles were used as the sacrificial templates to obtain hollow flower-like NiPdPt nanoparticles. NiPdPt nanoparticles were well assembled on the multiwalled-carbon nanotubes through electrostatic interaction. TEM, XRD and ICP-OES were used to characterize the structure and composition of the catalysts. The as prepared catalysts show excellent catalytic activity which is much better than the commercial ETK-Pd/C for ethanol electrooxidation in alkaline condition, presenting wide potential application for DEFCs in the future.

Acknowledgments

The authors acknowledge the financial support of National Natural Science Foundation of China with Grant Nos. 21190040, 21105095 and 91227114 and 973 projects (Nos. 2010CB933600).

References

[1] Z. Liu, B. Zhao, C. Guo, Y. Sun, Y. Shi, H. Yang, Z. Li, J. Colloid Interface Sci. 351 (2010) 233–238.
[2] S. Guo, S. Dong, E. Wang, Energy Environ. Sci. 3 (2010) 1307–1310.
[3] A. Brouzgou, A. Podias, P. Tsiakaras, J. Appl. Electrochem. 43 (2012) 119–136.
[4] A. Brouzgou, S.Q. Song, P. Tsiakaras, Appl. Catal. B Environ. 127 (2012) 371–388.
[5] C. Bianchini, P.K. Shen, Chem. Rev. 109 (2009) 4183–4206.
[6] S.Y. Shen, T.S. Zhao, J.B. Xu, Y.S. Li, J. Power Sources 195 (2010) 1001–1006.
[7] S. Sun, Z. Jusys, R.J. Behm, J. Power Sources 231 (2013) 122–133.
[8] J.W. Hong, D. Kim, Y.W. Lee, M. Kim, S.W. Kang, S.W. Han, Angew. Chem. Int. Ed. 50 (2011) 8876–8880.
[9] M. Shao, T. Yu, J.H. Odell, M. Jin, Y. Xia, Chem. Commun. 47 (2011) 6566–6568.
[10] H. Zhang, M. Jin, H. Liu, J. Wang, M. Kim, D. Yang, Z. Xie, J. Liu, Y. Xia, ACS Nano 10 (2011) 8212–8222.
[11] C. Zhu, S. Guo, S. Dong, J. Mater. Chem. 22 (2012) 14851–14855.
[12] S. Xie, N. Lu, Z. Xie, J. Wang, M.J. Kim, Y. Xia, Angew. Chem. Int. Ed. 51 (2012) 10266–10270.
[13] F. Hu, F. Ding, S. Song, P.K. Shen, J. Power Sources 163 (2006) 415–419.
[14] Q. He, W. Chen, S. Mukerjee, S. Chen, F. Laufek, J. Power Sources 187 (2009) 298–304.
[15] W. Du, K.E. Mackenzie, D.F. Milano, N.A. Deskins, D. Su, X. Teng, ACS Catal. 2 (2012) 287–297.
[16] Z. Zhang, L. Xin, K. Sun, W. Li, Int. J. Hydrogen Energy 36 (2011) 12686–12697.
[17] K. Lee, S.W. Kang, S.U. Lee, K.H. Park, Y.W. Lee, S.W. Han, ACS Appl. Mater. Inter. 4 (2012) 4208–4214.
[18] H.M. Song, B.A. Moosa, N.M. Khashab, J. Mater. Chem. 22 (2012) 15953–15959.
[19] S.T. Nguyen, H.M. Law, H.T. Nguyen, N. Kristian, S. Wang, S.H. Chan, X. Wang, Appl. Catal. B Environ. 91 (2009) 507–515.
[20] C. Zhu, S. Guo, S. Dong, Adv. Mater. 24 (2012) 2326–2331.
[21] X. Huang, Y. Li, H. Zhou, X. Duan, Y. Huang, Nano Lett. 12 (2012) 4265–4270.
[22] X. Yu, D. Wang, Q. Peng, Y. Li, Chem. Commun. 47 (2011) 8094–8096.
[23] Y. Hu, Q. Shao, P. Wu, H. Zhang, C. Cai, Electrochem. Commun. 18 (2012) 96–99.
[24] S.J. Bae, S.J. Yoo, Y. Lim, S. Kim, Y. Lim, J. Choi, K.S. Nahm, S.J. Hwang, T.-H. Lim, S.-K. Kim, P. Kim, J. Mater. Chem. 22 (2012) 8820–8825.
[25] D. Lee, H.Y. Jang, S. Hong, S. Park, J. Colloid Interface Sci. 388 (2012) 74–79.
[26] Y. Kim, H.J. Kim, Y.S. Kim, S.M. Choi, M.H. Seo, W.B. Kim, J. Phys. Chem. C 116 (2012) 18093–18100.
[27] B. Liu, H.Y. Li, L. Die, X.H. Zhang, Z. Fan, J.H. Chen, J. Power Sources 186 (2009) 62–66.
[28] Z. Liu, X. Zhang, L. Hong, Electrochem. Commun. 11 (2009) 925–928.
[29] A.V. Tripkovic, K.Dj. Popovic, J.D. Lovic, Electrochim. Acta 46 (2001) 3163–3173.
[30] S.C. Lai, M.T. Koper, Phys. Chem. Chem. Phys. 11 (2009) 10446–10456.
[31] S.C.S. Lai, S.E.F. Kleijn, F.T.Z. Öztürk, V.C. van Rees Vellinga, J. Koning, P. Rodriguez, M.T.M. Koper, Catal. Today 154 (2010) 92–104.
[32] L. Ma, D. Chu, R. Chen, Int. J. Hydrogen Energy 37 (2012) 11185–11194.
[33] R.C. Cerritos, M. Guerra-Balcázar, R.F. Ramírez, J. Ledesma-García, L.G. Arriaga, Materials 5 (2012) 1686–1697.
[34] Z.X. Liang, T.S. Zhao, J.B. Xu, L.D. Zhu, Electrochim. Acta 54 (2009) 2203–2208.
[35] W. Yang, X. Wang, F. Yang, C. Yang, X. Yang, Adv. Mater. 20 (2008) 2579–2587.